Contract No:

This document was prepared in conjunction with work accomplished under Contract No. DE-AC09-08SR22470 with the U.S. Department of Energy.

Shielding and Detector Response Calculations Pertaining to Category 1 Quantities of Plutonium and Hand-Held Plastic Scintillators

A.H. Couture – Savannah River National Laboratory

Abstract

Nuclear facilities sometimes use hand-held plastic scintillator detectors to detect attempts to divert special nuclear material in situations where portal monitors are impractical. MCNP calculations have been performed to determine the neutron and gamma radiation field arising from a Category 1 quantity of weapons-grade plutonium in various shielding configurations. The shields considered were composed of combinations of lead and high-density polyethylene such that the mass of the plutonium plus shield was 22.7 kilograms. Monte-Carlo techniques were also used to determine the detector response to each of the shielding configurations. The detector response calculations were verified using field measurements of high-, medium-, and low- energy gamma-ray sources as well as a Cf-252 neutron source.

Introduction

The Nuclear Regulatory Commission defines a Category 1 quantity of plutonium as more than two kilograms. In certain situations, in lieu of portal monitors, hand-held plastic scintillators are used to detect attempts to divert special nuclear material. These scintillators are sensitive to both gamma and neutron radiation. MCNP [1] simulations have been produced to calculate the response of a common hand-held plastic scintillator, the PRM-470B from TSA systems [2], to a Category 1 quantity of weapons-grade plutonium (WGPu) in various shielding configurations. A two kilogram sphere of metallic plutonium has a radius of 2.887 cm, the size of a racquetball. The shielding configurations modeled consisted of lead and/or high-density polyethylene in spherical shells perfectly encasing the WGPu. The mass of the plutonium plus the shield was fixed at 22.7 kilograms (50 lbs). This mass was chosen from OSHA standards as the maximum a worker can lift safely without injury. The shielding configurations investigated are listed in Table 1 along with their dimensions. In all simulations, count rates in the PRM-470B were calculated assuming that the detector was held with its face pointed towards the center of the plutonium mass at a distance of two feet from the surface of the shielding. This is a conservative estimate, since in practice the detector is typically held at the surface of the object being monitored. The intensity of radiation field is approximately inversely proportional to the square of the distance from the source. Thus, count rates in a detector held at the surface of the shielding should be at least a factor of ten greater than those reported at two feet.

Radiation Transport

The MCNP simulation for each shielding configuration was broken into three components: gamma radiation arising from the decay of WGPu, neutron radiation, and gamma radiation induced by neutron reactions in the WGPu and shielding material. Since the hand-held detector does not contain any electronics capable of spectroscopy or particle identification, the count rates calculated from each part of the simulation were summed to obtain the overall detector response.

Shield Configuration	Inner Layer Radius (cm)	Outer Radius (cm)
100% Pb	N/A	7.72
25% Pb_i – 75% $Poly_o$	5.11	15.93
25% Pb_o – 75% $Poly_i$	15.78	15.93
50% Pb_i – 50% $Poly_o$	6.23	14.17
50% Pb_o – 50% $Poly_i$	13.80	14.17
75% Pb_i – 25% $Poly_o$	7.05	11.82
75% Pb_o – 25% $Poly_i$	10.98	11.82
100% Poly	N/A	17.36

Table 1: Shield thickness calculated such that the weight of the shield and plutonium is 50 pounds. The column labeled shield configuration gives the weight percent of each shielding material. The subscripts "i" and "o" denote which material constitutes the inner and outer layer of the shield, respectively.

Gamma Radiation

Since ^{239}Pu constitutes the bulk of WGPu, the first simulations only took gamma radiation produced during its decay into account. Subsequent simulations included all major isotopes found in WGPu. Gamma activity increases for many years after initial production from the ingrowth of ^{241}Am. The simulated WGPu was decay corrected to ten years after separation. Gamma libraries containing the energies and branching ratios for the gamma-rays produced by each isotope were taken from the National Nuclear Data Center database [3]. Any gammas with energies less than 20 keV were not simulated, since they are below the detection threshold. The gamma library for each isotope was sampled based upon its relative gamma output above this threshold, taking into account mass fraction, specific activity, and the number of gammas produced per decay. Table 2 shows these parameters and the percent of events in the simulations that were sampled from each isotope. While Table 2 indicates that only slightly more than one percent of the total gamma-ray output of ten-year-old WGPu is produced by 239Pu with the vast majority of gamma-rays arising from ^{241}Am and ^{237}U, the ^{239}Pu gamma-rays have a considerably higher average energy and are more penetrating.

Isotope	Decayed Mass (%)	Sp. Activity (Ci/g)	γ/Decay ($E_\gamma > 20$ keV)	Relative γ Production (%)
^{238}Pu	0.0148	17.1	4.7×10^{-4}	0.031
^{239}Pu	93.538	0.062	7.0×10^{-4}	1.056
^{240}Pu	5.827	0.227	5.2×10^{-4}	0.180
^{241}Pu	0.345	0.251*	1.5×10^{-5}	< 0.001
^{242}Pu	0.062	0.004	4.0×10^{-4}	< 0.001
^{241}Am	0.213	3.428	3.8×10^{-1}	72.837
^{237}U	Trace	N/A	1.15	25.896

Table 2: Parameters used in gamma radiation source calculations. The asterisk beside the specific activity of ^{241}Pu indicates that only the alpha-decay branch of its decay scheme is included in this chart, since the beta-decay branch does not produce gamma-rays.

As photons travel through the WGPu and shielding material, they interact by either the photoelectric effect or Compton scattering. In both cases, energy is transferred to electrons. While these electrons are not directly tracked in the simulation, they create additional photons through bremsstrahlung and atomic fluorescence that are tracked. The simulations attempt to estimate how many photons exit the shielding material; however a good shield will stop most photons. To treat them as nature does is inefficient. MCNP allows variance reduction techniques that decrease the time required to obtain precise answers [1]. The shields were divided into layers. As photons pass through a particular layer, some are stopped. The surviving photons are then split into enough new photons to maintain the original population, while lowering the weight each photon contributes to the final answer by a compensatory ratio without changing their energy distributions. A similar technique was used to handle the dominant 59.6 keV gamma-ray emitted by ^{241}Am. More than 93% of the photons above 20 keV emitted by ^{241}Am occur at this energy, however these are easily shielded and will not contribute greatly to the results of the simulations. The sampling rate for this gamma-ray was decreased by a factor of 10, while the relative weighting of contributions to the calculated gamma flux arising from these gammas was increased by a factor of 10.

Neutron Radiation

Plutonium isotopes with even mass numbers generate neutrons at high rates through spontaneous fission. The most plentiful of these isotopes in WGPu is ^{240}Pu, by far. Source neutrons were generated uniformly throughout the plutonium mass. The energy distribution of the source neutrons used in the MCNP simulations was determined by the Watt fission spectrum for ^{240}Pu, given by:

$$P(E) = Cexp(-E/a)\sinh(\sqrt{bE}),$$

where a = 0.799 MeV, b = 4.903 MeV^{-1}, and C is a normalization constant [4]. The overall spontaneous fission rate of the source was determined by the amount of ^{238}Pu, ^{240}Pu, and ^{242}Pu in the modeled item, as well as the spontaneous fission rate and multiplicity distribution for each of these isotopes. The neutron emission rate from spontaneous fission used in the calculations was 1.22×10^5 neutrons/s. Additional neutrons are generated in the simulations through neutron-induced fission primarily by ^{239}Pu and ^{241}Pu, as well as $(n,2n)$ reactions in the WGPu and lead shielding. Most neutrons resulting from fission reactions are emitted essentially instantaneously, however approximately 1% of neutrons are delayed following the beta decay of certain fission products. Delayed neutrons were not included in these MCNP simulations. Metallic plutonium may also emit neutrons at low rates through (α,n) reactions arising from low-Z impurities. These neutrons were not included in the simulations either. Neutron radiation is shielded much more effectively by polyethylene than by lead. Elastic collisions with hydrogen nuclei in the polyethylene slow the neutrons to thermal energies, at which point they may be captured in (n,γ) reactions. Surrounding WGPu with lead and/or polyethylene will not necessarily decrease the neutron radiation field. Neutrons that have been reflected back into the WGPu by the shielding can induce fission reactions and actually increase the magnitude of the radiation field outside the shielding.

Neutron-Induced Gamma Radiation

Fission, neutron capture, and inelastic scattering are often accompanied by the emission of gamma radiation. Delayed gamma radiation is also produced by fission products that accumulate in the

WGPu. Gamma-rays produced by fission products and prompt gamma-rays from spontaneous fission are not modeled in the MCNP simulation. The most important neutron-induced gamma-rays for these shielding calculations are the 2615, 583, and 860 keV gamma-rays produced by inelastic scattering with ^{208}Pb and the 2223 keV capture gamma from ^{1}H. When considering thick lead shielding, these gamma-rays are more important than the gammas arising directly from the decay of the WGPu.

Detector Response

The TSA Model PRM-470B Portable Radiation Monitor is a light-weight (1.25 kg), portable, hand-held unit designed to detect radioactive materials [2]. The detector contains a polyvinyl toluene (PVT) plastic scintillator with dimensions of 3.1 cm x 8.8 cm x 7.2 cm. The detector operates in two modes: background mode and search mode. When the detector is powered up, it takes an initial background count and stores the count rate. The detector then transitions to search mode where the count rate is measured in 50 ms intervals. The most recent eight of these intervals are averaged and this moving average is compared to the alarm threshold. If the threshold is exceeded, an audible alarm is produced. The alarm threshold is determined by the stored background count rate (*BKG*) and a sensitivity setting (*n*) using the following formula:

$$Alarm\ Level\ = \left(n \cdot \sqrt{BKG}\right) + BKG.$$

The sensitivity setting is controlled by an internal rotary switch located on the circuit board and may vary between 0.1 and 10 [3]. The factory default sensitivity is 3, the level recommended by the manufacturer.

<u>Photon Response</u>

All photons that enter the plastic scintillator do not induce a response from the detector. The probability of a photon that enters the detector being detected depends on the energy of the photon. This probability is called the detector efficiency (ε). The radiation transport calculations performed determined the number of photons per unit time that entered the detector as a function of energy. Separate MCNP calculations were performed to evaluate the detector efficiency of the plastic scintillator. There is a fixed discriminator level in the detector electronics to filter out electronic noise. This discriminator prevents photons that deposit less than 20 keV of energy into the scintillator from registering counts. There is also a 3 mm polycarbonate shell that encases the detector through which photons must pass. The energy-dependent attenuation (α) of photons traversing this shell was also calculated using MCNP. The total count rate (*C*) can be derived from photon current (*N*) entering the detector using the following equation:

$$C = \sum_{E>20\ keV} N_E \varepsilon_E (1 - \alpha_E),$$

where the subscript, E, denotes that the photon current, detector efficiency, and attenuation pertain to a particular energy bin. A graph of the detector efficiency is shown in Figure 1.

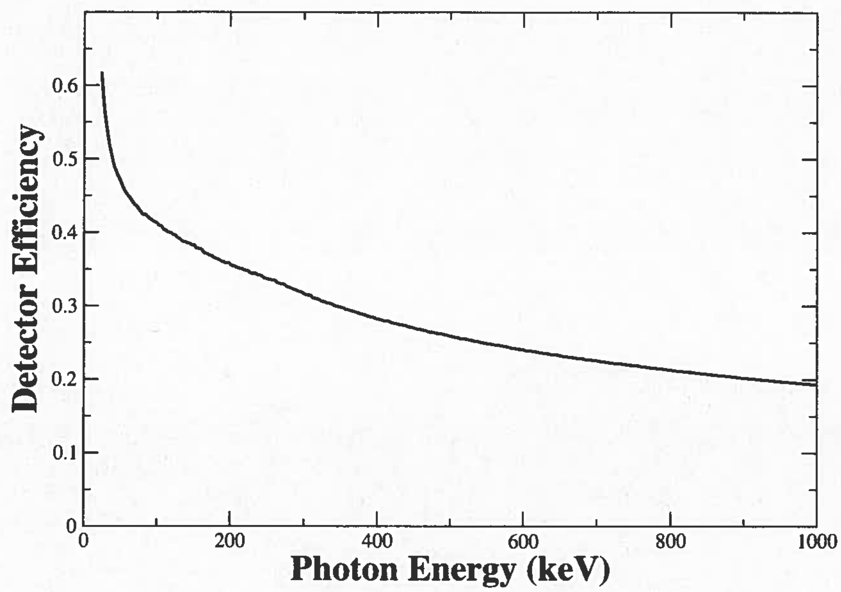

Figure 1. PVT detector efficiency for photons.

Neutron Response

While photons primarily interact with the hydrogen and carbon of the scintillator through Compton scattering with atomic electrons, neutrons interact with the nuclei through elastic and inelastic scattering as well as (n,γ) reactions. The most important mechanism in these simulations is elastic scattering by fast neutrons on hydrogen nuclei. The light output of the scintillator is different for photon and neutron interactions arising from differences in the ionization power of the scattered electrons and protons. If either a photon or a neutron deposits a large amount of energy into the scintillator, the different ionization powers are insignificant; both events will register a count in the detector. However, determining the threshold energy deposition for neutrons that corresponds to the 20 keV photon threshold is important for these calculations. According to measurements by Stevanato [4] and Pozzi [5] with similar plastic scintillators, the light output of a 20 keV electron corresponds to that of a 150-275 keV proton. To be conservative, the MCNP detector response calculations used 275 keV as the energy deposition threshold for neutron detection.

Performance Testing

The photon and neutron response of the PRM-470B was performance tested by comparing count rates measured at four distances using four sources with MCNP predictions. The radionuclides used were: ^{133}Ba with photon emissions at several energies between 30 and 384 keV, ^{137}Cs with a gamma line at 661 keV, ^{60}Co with two gammas at 1173 and 1332 keV, and the spontaneous fission neutron emitter, ^{252}Cf. The count rate was measured at distances of 50, 75, 100, and 150 cm from each source. Background count rates were measured several times over the course of the performance test. The PRM-470B was operated in background mode for all measurements, which means the detector would average the count rate over 10 seconds and then display the count rate on its screen.

Twelve measurements were taken for each source-distance combination and the standard deviation of these measurements was used as the statistical uncertainty. The sources of systematic uncertainty were the source activity (3%), the effective solid angle (2%), and material composition and density (2%).

All measured count rates were higher than predicted. Photons and gammas scattering into the detector from the walls, table, and other surrounding material was a significant effect. The table upon which the sources and detector were placed was included in the MCNP simulation. The walls, detector electronics, and computer were not. For the photon measurements, the predicted and measured count rates differed by less than 30%. The magnitude of the discrepancy was larger for higher energy gamma rays, indicating that the likely cause was inscattering from materials not included in the simulation. Figure 2 shows the results of the gamma measurements compared with prediction made using MCNP. The neutron measurement had a larger discrepancy, as shown in Figure 3. Measured count rates exceeded the predicted count rates by approximately a factor of two. The effect of the neutron energy deposition threshold was tested by lowering from 275 keV to 150 keV, reducing the discrepancy to roughly a factor of 1.5. Since the count rate was considerably higher than predicted for neutrons, the PRM-470B will be more effective at detecting shielded plutonium than the MCNP modeling suggests. Likewise, neutrons and photons scattered off objects in the room were included in the modeling for the performance test, however the MCNP models for the shielded plutonium did not contain any material other than the scintillator, plutonium, and shielding. Room return radiation is a significant effect, increasing the sensitivity of the detector relative to the modeled predictions.

Results

Background measurements taken using the PRM-470B at various locations around the Savannah River Site resulted in approximately 100 cps. At this background level, the detector will alarm if the average count rate exceeds 130 cps with the factory default alarm level. Initial simulations that considered only the gamma-rays produced by ^{239}Pu are summarized in Table 3. These simulations show that a pure polyethylene shield as well as the configurations where polyethylene is surrounded by a lead layer will undoubtedly set off the detector's alarm. Configurations with an inner lead shield gave inconclusive results and further modeling was required taking into account gamma emissions from other isotopes as well as neutron emissions.

When the gamma emissions from all plutonium isotopes as well as ^{241}Am and ^{237}U were included in the simulations, the calculated gamma radiation field outside the shielding nearly doubled. However, this was not enough to surpass the 30 cps alarm threshold to reliably detect a diversion attempt. When neutrons and neutron-induced gamma-rays were included, all shielding configurations examined surpassed the alarm threshold at a 2 ft standoff. The optimal shielding configuration is nearly 50% lead and 50% polyethylene by mass with the lead being the inner layer. These results are summarized in Table 4.

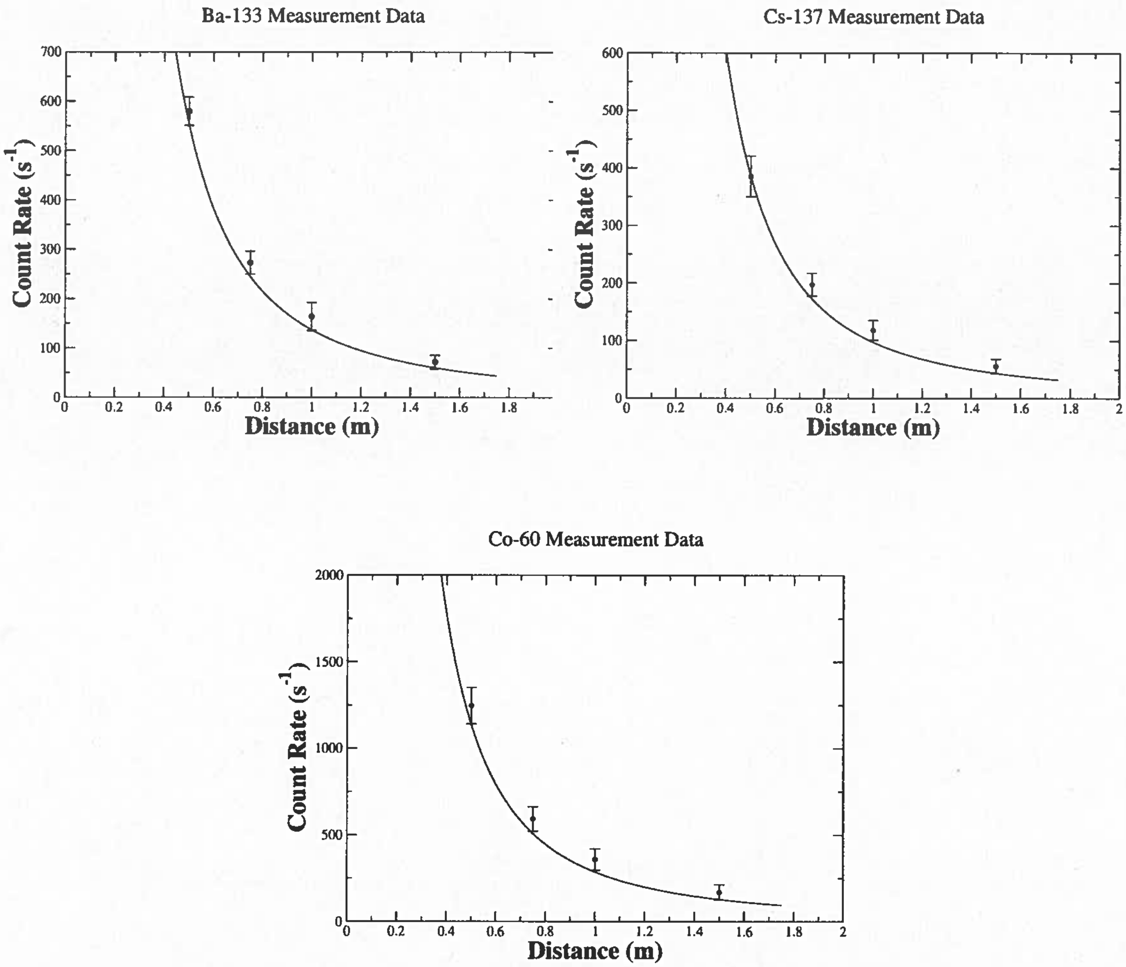

Figure 2: Comparison between the count rates predicted by MCNP (solid lines) and measurements made with the PRM-470B (data points) for the gamma sources used in the performance test. Error bars represent both systematic and statistical uncertainties and are reported at 2σ.

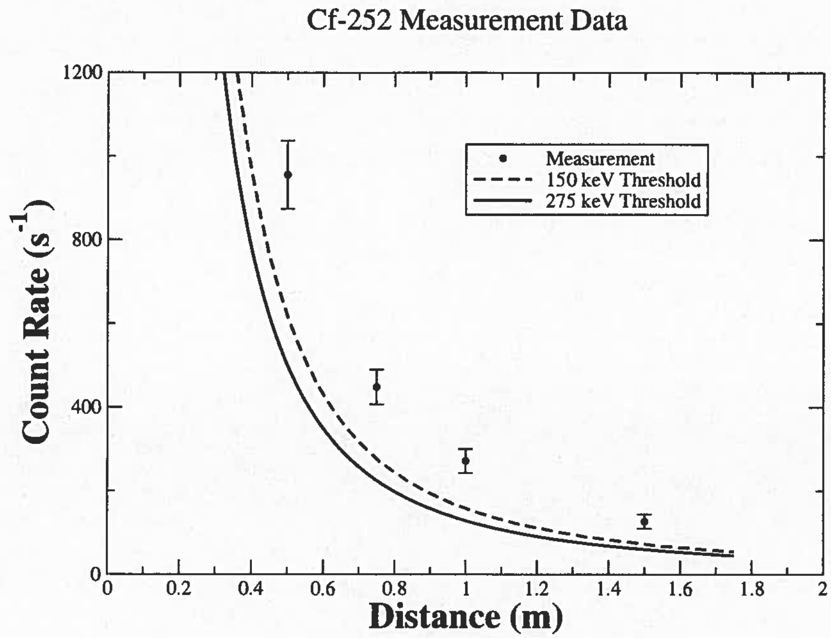

Figure 3: Comparison between the count rate predicted by MCNP with a 275 keV neutron energy deposition threshold (solid line), a 150 keV energy deposition threshold (dashed line) and measurements made with the PRM-470B (data points) for the Cf-252 source used in the performance test. Error bars represent both systematic and statistical uncertainties and are reported at 2σ.

Shielding Configuration	Count Rate at 2 ft (cps)
No shield	11000
100% Pb	0.6
25% Pb_i – 75% $Poly_o$	16
25% Pb_o – 75% $Poly_i$	1140
50% Pb_i – 50% $Poly_o$	3
50% Pb_o – 50% $Poly_i$	630
75% Pb_i – 25% $Poly_o$	1.2
75% Pb_o – 25% $Poly_i$	250
100% Poly	6400

Table 3: Predicted count rates for the PRM-470B at 2 ft from the surface of the object arising from gamma-rays emitted by 239Pu only. The column labeled shield configuration gives the weight percent of each shielding material. The subscripts "i" and "o" denote which material constitutes the inner and outer layer of the shield, respectively.

These calculations indicate that scanning with a hand-held plastic scintillation detector is an effective countermeasure to prevent the diversion of a Category 1 quantity of WGPu from a nuclear facility. While the calculated count rates are the same order of magnitude as the alarm level, the assumptions that the simulations are based upon are quite conservative, particularly the two foot standoff distance. If the count rate is calculated at the surface of the shield, where it is measured in practice, the 50% lead - 50% poly configuration produces 1500 cps rather than the 54.5 cps reported. When scanning items with a hand-held plastic scintillator, the initial background reading of the detector should be noted. Elevated background readings alter the sensitivity of the detector and are cause for concern.

Shielding Configuration	Gamma (cps)	Neutron (cps)	(n,γ) (cps)	Total (cps)
100% Pb	1.2	110	2.6	113.8
25% Pb – 75% Poly	25	13	41	79
50% Pb – 50% Poly	5.5	24	25	54.5
75% Pb – 25% Poly	2.1	47	11	60.1

Table 4: Predicted count rates for the PRM-470B at 2 ft from the surface of the object arising from decay gammas, neutrons, and neutron-induced gammas emitted by all isotopes found in WGPu. The column labeled shield configuration gives the weight percent of each shielding material. In each of these shielding configurations, lead is the inner shield.

References

[1] X-5 Monte Carlo Team, "MCNP – A General N-Particle Transport Code, Version 5 Volume I: Overview and Theory", LA-UR-03-1987 (2003).

[2] PRM-470B Operating And Service Manual. TSA Systems, Ltd. Version 1.06 (2002).

[3] M.B. Chadwick, *et al.* "ENDF/B-VII.1 Nuclear Data for Science and Technology: Cross Sections, Covariances, Fission Product Yields and Decay Data." Nuclear Data Sheets. Volume 112, Issue 12. (2011), 2887–2996.

[4] L. Stevanato, *et al.* "Light Output of EJ228 Scintillation Neutron Detectors." Applied Radiation and Isotopes. Volume 69. (2011), 369-372.

[5] S.A. Pozzi, J.A. Mullens, and J.T. Mihalczo. Analysis of Neutron and Photon Detection Postion for the Calibration for Plastic (BC-420) and Liquid (BC-501) Scintillators. ORNL/TM2003/168. (2003).